Research Article | Vol. 26, No. 25 | 10 Dec 2018 | OPTICS EXPRESS 33148
Optics EXPRESS

Polarizing beam splitter integrated onto an optical fiber facet

VINCENT HAHN,[1,2,4,*] SEBASTIAN KALT,[1,4] GAYATHRI M. SRIDHARAN,[3] MARTIN WEGENER,[1,2] AND SHANTI BHATTACHARYA[3]

[1]*Institute of Applied Physics, Karlsruhe Institute of Technology, Wolfgang-Gaede-Str. 1, 76131 Karlsruhe, Germany*
[2]*Institute of Nanotechnology, Karlsruhe Institute of Technology, P.O. Box 3640, 76021 Karlsruhe, Germany*
[3]*Department of Electrical Engineering, Indian Institute of Technology Madras, Chennai 600036, India*
[4]*These authors have contributed equally to this work.*
[*]*vincent.hahn@kit.edu*

Abstract: When light either leaves or enters an optical fiber, one often needs free-space optical components to manipulate the state of polarization or the light's phase profile. It is therefore desirable to integrate such components onto a fiber end facet. In this paper, we realize, for the first time, a polarizing beam splitter fabricated directly onto the end facet of a single-mode optical fiber. The element is composed of a refractive prism, intentionally slightly displaced from the core of the fiber, and an elevated and suspended sub-wavelength diffraction grating, the lamellae of which have an aspect ratio of about 5. This integrated micro-optical component is characterized experimentally at 1550 nm wavelength. We find that the two emerging output beams exhibit a degree of polarization of 81 percent and 82 percent for Transverse Magnetic (TM) and Transverse Electric (TE) polarization, respectively.

1. Introduction

Optical fibers have become ubiquitous. In many situations, they have replaced bulky free-space optics. However, as long as not all functionalities have been integrated into fiber optics, interfaces to free-space optics are crucial components. This necessity has spurred research towards micro-optical components with increasing sophistication, directly fabricated on the end facets of optical fibers (as reviewed in [1]). Early work started with essentially planar structures, while more recent studies have arrived at complex three-dimensional (3D) architectures. The following paragraph reviews examples of micro-optical components, all manufactured directly on optical fiber end facets.

Early on, diffractive optical elements for focusing and beam shaping have been realized by using electron-beam lithography (EBL) [2]. This allowed for generating a rectangular far-field focus without any free-space components. More recent EBL work [3] demonstrated refractive-index sensors based on gold nanotrimers. A polarizing diffraction grating was milled on the facet of an optical fiber of a high-power fiber laser by using focused ion beam milling (FIB) [4]. Efficient fiber-to-waveguide coupling was achieved by fabricating a Fresnel lens on the end of an optical fiber by FIB [5]. Furthermore, using FIB, an axicon lens on an optical fiber was fabricated. This axicon was successfully applied for optical tweezing [6]. Vortex-beam generators were created by FIB as well [7], but also by using 3D direct laser writing (DLW) [8], sometimes also referred to as laser direct writing, two-photon lithography, or 3D micro- or nanoprinting [9]. DLW provides complete freedom for the making of 3D architectures, but is more limited with respect to spatial resolution compared to EBL and FIB. Nevertheless, combinations of 3D woodpile photonic crystals and refractive focusing lenses have served as early proof-of-principle demonstrations [10]. Micro-lenses made by DLW

#347019 https://doi.org/10.1364/OE.26.033148
Journal © 2018 Received 28 Sep 2018; revised 23 Oct 2018; accepted 23 Oct 2018; published 4 Dec 2018

Optics EXPRESS

have also been presented in [11]. In addition, an integrated microfluidic device for single-cell trapping and spectroscopy has been realized by DLW [12]. This device was based on four total-internal reflection prisms, arranged on the fiber end facet. Later, doublet and triplet refractive micro-lens systems have been fabricated on fiber end facets for sensing applications [13]. With the same DLW approach, phase masks for shaping doughnut and top-hat beam profiles have been demonstrated as well [14]. Microstructured gradient-index antireflective coatings made by DLW [15] can also be integrated onto the end facet of optical fibers. Finally, in addition to all of these passive elements, active temperature sensors on fiber end facets based on up-conversion luminescence have been realized by DLW, too [16]. Further fabrication approaches suitable for the making of micro-optical elements on the end facet of a fiber, such as self-assembly, soft imprinting, projection lithography, holographic lithography, and hybrid techniques have also been reviewed recently [1] together with potential applications of the resulting devices.

On this basis, the question arises: Can all kinds of devices known from free-space optics be integrated directly on top of the end facet of an optical fiber? For example, one element missing so far is a polarization-dependent beam splitter. The novelty of our present work lies in that we design, realize, and characterize experimentally such a micro-optical element. For the fabrication, we choose DLW, allowing to manufacture the entire device on the end facet of a single-mode optical fiber within just a few minutes time.

The integrated polarizing beam splitter presented here can be applied in different ways. For example, it can simply serve as a polarizer for light impinging from the fiber side. In contrast to the integrated polarizer discussed above [4], however, the polarizing beam splitter does not reflect the unwanted component, which may lead to undesired feedback into the laser light source. Using the element in the reverse direction, *i.e.*, for light impinging from the air side, yields additional application possibilities. For example, the optical power of two orthogonally polarized beams at the same wavelength can be coupled into the fiber mode simultaneously. Apart from reflection losses, no power would be lost (unlike for a non-polarizing beam splitter).

2. Theory

The polarization beam splitter is basically a sub-wavelength lamellar grating, as shown in Fig. 1. Such gratings can have high aspect ratios, with w being the ridge width, h the grating height and d the period. Following earlier work [17,18], we use the modal method to design the ridge width, the period, and the effective indices. The grating is designed such that only three modes exist, namely the fundamental Transverse Magnetic (TM) mode and two Transverse Electric (TE) modes, with effective indices $n_{\mathrm{eff1(TE)}}$ and $n_{\mathrm{eff2(TE)}}$, respectively. The former couples into the zeroth order, whereas, if the height of the grating is chosen to satisfy

$$\left|n_{\mathrm{eff1(TE)}} - n_{\mathrm{eff2(TE)}}\right| \frac{h}{\lambda} = \frac{2q-1}{2}; q = 1, 2, ..., \tag{1}$$

the two TE modes will couple into the -1st order. The grating height can be calculated from Eq. (1), and clearly depends on the values of the effective indices of the two TE modes. Those values are, in turn, controlled by the values of the incidence angle, fill factor $f = w/d$, period d, and of course, the ridge and groove refractive indices n_{r} and n_{g}, respectively. In our case, the groove is simply an air void. Using this technique, the design arrived at is presented in Table 1. These values result in an aspect ratio of 4.72 and a fill factor of 0.4. The design was carried out assuming that the grating is illuminated at the Littrow angle. In this case, the angle of incidence was found to be $56.3°$. The real usefulness of the DLW technique for this application becomes apparent if one takes the angle of incidence into account. If the lamellar grating was meant to have light incident normally on it, then it could

have been written directly on the fiber tip by aforementioned lithography methods without 3D printing capabilities, *e.g.* FIB or EBL. However, in this specific case, the light has to be incident under an angle that is quite large (see Table 1).

Figure 2 shows a scheme of the overall arrangement. A total internal reflecting prism is directly written onto the core of the fiber. The apex of the prism is intentionally offset by $7\,\mu m$ from the fiber's center in the positive x direction. The internal angles of the prism are chosen such that the beam impinges onto the lamellar grating at an angle of $56.3°$ and that the condition for total internal reflection is fulfilled at the first polymer-air interface. In addition, the beam should exit the prism at the second polymer-air interface at normal incidence to minimize reflection losses, resulting in a prism with a base of $33\,\mu m$ and base angles of $62°$ and $56°$ respectively. The structure is designed and optimized to work at the wavelength $\lambda = 1550\,nm$.

Table 1. Polarization splitting grating design parameters.

Parameter	n_r	n_g	w	d	h	λ	θ_i
Value	1.52	1	0.373 µm	0.932 µm	1.76 µm	1550 nm	56.3°

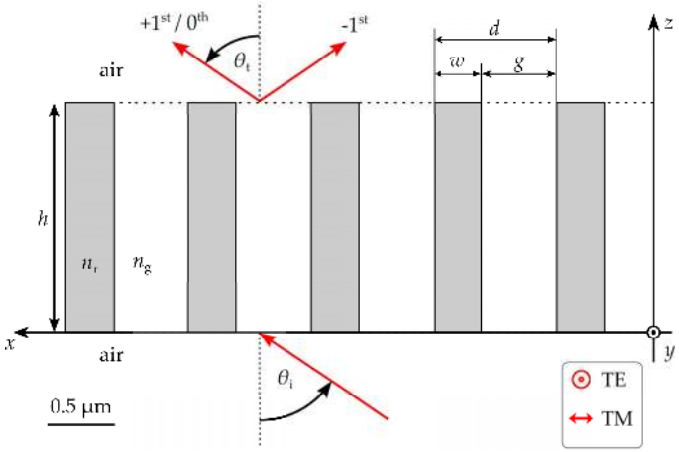

Fig. 1. Schematic of a sub-wavelength grating with period $d < \lambda$, where λ is the wavelength of the incident light. A design must arrive at the values of ridge width w, period d, and angle of incidence θ_i, in order to obtain the desired effective indices. The height h can then be calculated based on the polarization function to be realized.

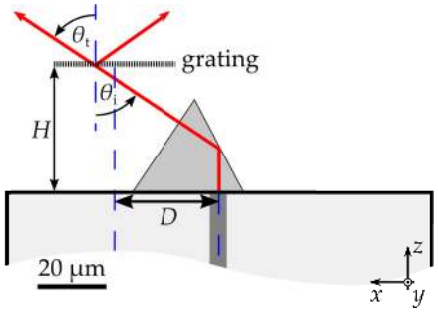

Fig. 2. Scheme of the prism that redirects the incident light to the polarizing beam splitter, with the correct angle of incidence θ_i. The height of the grating, H, and its center offset with respect to the fiber mode, D, are indicated.

Optics EXPRESS

The sub-wavelength grating is written parallel to the fiber end-facet, at a distance from the prism. A support structure (not shown in Fig. 2), which is a U-shaped profile with a wall thickness of $5\,\mu m$, is used to hold the grating at the required height. In the ray-optical approximation, the height and relative lateral position of the grating do not determine the performance, provided the grating is separated from the prism. In wave optics, however, the grating height and the grating position do enter because the Gaussian plane wave emerging from the fiber diverges away from the fiber end facet plane and gradually turns into a spherical Gaussian beam. Therefore, the grating position needs to be optimized. To perform this optimization, we have performed the numerical calculations described in the following section.

3. Numerical calculations

In previous systems employing large-aspect-ratio lamellar gratings fabricated by DLW, the achieved grating pitches were similar to the ones reported here. For example, Thiel et al. reported a ridge width of $0.44\,\mu m$ and a grating pitch of $13\,\mu m$, fabricated using a spun-on photoresist SU-8 [19]. However, the lamellae were sandwiched in between two stabilization layers.

The parameters given in Table 1 clearly show that the laser writing system has to be pushed to its resolution limits in order to achieve the desired effective indices. Therefore, simulations were carried out to not only validate the design, but also to analyze its sensitivity to small fabrication errors and further optimize the design.

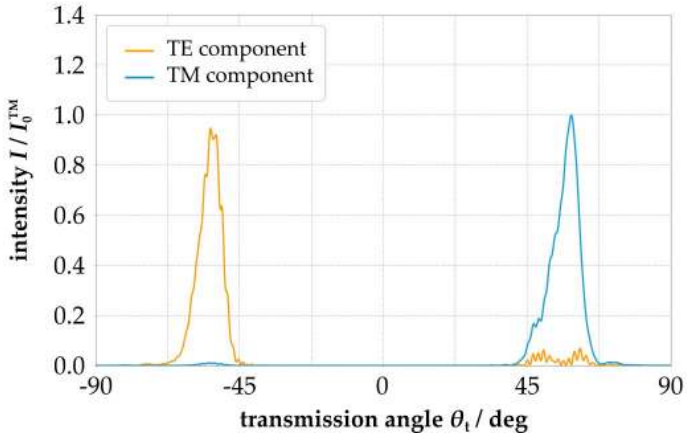

Fig. 3. Numerically calculated far-field intensity components behind the polarizing beam splitter structure as it would be measured in the experimental characterization setup. The structure is designed with the theoretical parameters presented in Table 1 and an optimized grating pitch of $d = 1.05\,\mu m$.

The multiphysics module of the simulation tool COMSOL™ was used to calculate the far-field pattern, results of which are shown in Fig. 3. Equal intensities of the TE and TM polarized mode were incident onto the prism at the fiber end facet. We found minimal crosstalk of the two modes when increasing the grating or lamella period from the value of $d = 0.938\mu m$ calculated by using modal theory (see section 2) to $d = 1.05\,\mu m$, while fixing the angle of incidence. The value of d is not critical: When changing d by $\pm 5\%$, the crosstalk does not increase considerably. The dependence on the lamella width w is quite weak. When changing w by $\pm 100nm$ with respect to design value (see Table 1) of $373\,nm$, the crosstalk barely changes. Likewise, the crosstalk hardly changes when varying the lamella

Optics EXPRESS

height h in the interval $[1700\ \text{nm}, 2200\ \text{nm}]$. As we will see below, the angle of incidence can easily be checked experimentally (see Fig. 7) to $\pm 1°$. Therefore we have not considered larger deviations in our numerical calculations. Regarding the position of the grating (see end of section 2), one would naively think that the optimum position of the grating is as close to the prism as geometrically possible (compare Fig. 2). However, our numerical calculations indicate that the optimal height is a bit larger. The optimum parameters are given by $H = 36\,\mu\text{m}$ and $D = 31.4\,\mu\text{m}$. The grating consists of 37 lamellae.

Figure 4 shows the path taken by TE and TM polarized light incident onto the prism. Calculations were also carried out with variations in the ridge width, from $373\,\text{nm}$ to $410\,\text{nm}$ (approximately a variation of 10%). It was observed that this change did not significantly affect the efficiency of the splitting.

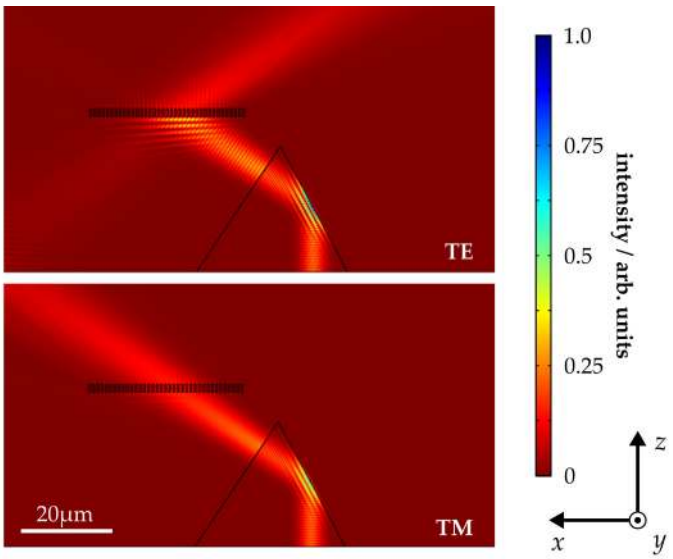

Fig. 4. Numerical calculations showing how the beam splitter affects the two polarizations, TE and TM. The corresponding parameters are summarized in Table 1, except for the optimized grating pitch ($d = 1.05\,\mu\text{m}$).

4. Fabrication and characterization setup

The 3D DLW process has been performed using a Photonic Professional GT (Nanoscribe GmbH) system employing a pulsed laser source, operating at $780\,\text{nm}$ center wavelength with a pulse duration around $100\,\text{fs}$ and a pulse repetition rate of $80\,\text{MHz}$. Furthermore, a custom objective lens (Zeiss LD LCI Plan-Apochromat 63x/1.2 Imm) was used. This objective lens has a correction collar for use with immersion liquids having a refractive index in the range of 1.43 to 1.52. Therefore, it is suitable for dip-in writing [20] in conjunction with most photoresists, which typically possess a refractive index around 1.47 in their liquid state. We chose IP-L 780 (Nanoscribe GmbH) as photoresist instead of the commonly used IP-Dip for its higher resolution and lower shrinkage. The photoresist was heated to $40°\text{C}$ before writing in order to fully dissolve any residual monomer aggregates.

We promoted adhesion of the polymer structures on the cleaved fiber's end facets using a silanization procedure. The $30\,\text{cm}$ long pieces of standard SMF-28 fiber were mounted on a custom-made sample holder. The objective lens was manually centered on the fiber core while illuminating the loose end with a white-light source. The structure was then written at a writing speed of $10\,\text{mm/s}$, which results in a total writing time of less than 90 seconds. A laser power of $20\,\text{mW}$, measured at the entrance pupil of the objective lens, was used. For

Optics EXPRESS

the prism and support, a hatching and slicing distance of 120 nm and 300 nm was chosen, respectively. The lamellae were sliced 20 times with a distance of 20 nm . Laterally, the individual lamellae consist of single voxel lines. The subsequent development step was carried out in a bath of Acetone (10 minutes) and 2-Propanol (1 minute).

After fabricating such a polarization manipulating structure on a fiber tip, the functionality of the structure has been characterized in the setup illustrated in Fig. 5. The setup consists of several major parts as described in the following paragraphs.

The first part relates to the generation of an arbitrarily polarized input signal. In our case, we used an InGaAsP laser diode with a transmission maximum at 1550 nm . The laser diode is driven with a laser diode driver (Newport 501B). The slightly elliptically polarized signal is coupled through single mode fibers into a fiber polarization controller (Thorlabs FPC030). This allows the polarization of the propagating mode to be set to any arbitrary state.

The signal, with desired polarization, is coupled into one end of a bare fiber that has the fabricated structure or the device under test (DUT) on the other end. This is done using a PC/PC mating sleeve and a bare fiber terminator (Thorlabs BFT1) including the respective fiber connector (Thorlabs B30126C3). An immersion fluid has been used to improve the fiber's coupling efficiency. The fiber end with the DUT is mounted in a rotatable fiber clamp (Thorlabs SM1F1-250). Consequently, the fiber end (and the DUT) can be rotated until the transmission orders lie in a plane parallel to the optical table. This can be achieved using a movable camera system, which also helps in centering the fiber at the pivot point. The CMOS-camera is therefore mounted on a 3D translational stage and can be pivoted within a range of 180° .

After aligning the fiber, the camera system can easily be substituted by an optical analysis setup. The transmitted light is collected and collimated by a plano-convex lens with its focal point at the center of rotation. The incoming polarization is analyzed using a rotatable linear dichroic film polarizer (Thorlabs LPIREA050-C). After the polarizer, the light is focused onto an InGaAs photodiode, using another plano-convex lens. The position of the photodiode can be shifted in the *xy* -plane to compensate for off-axis fiber tips.

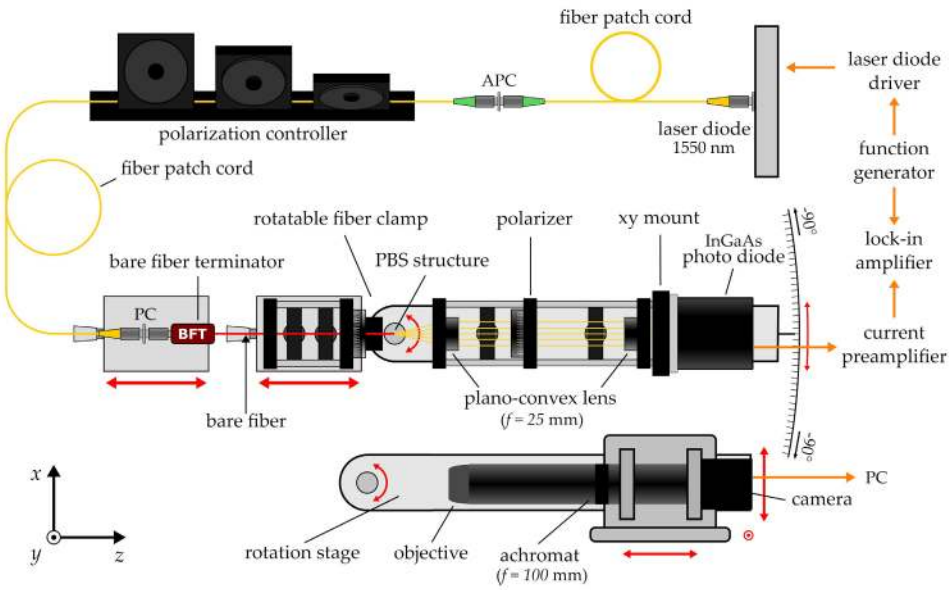

Fig. 5. Experimental setup for the characterization of a polarization manipulating sub-wavelength structure on a fiber's facet.

Optics EXPRESS

The final part of the setup includes the electronic evaluation of the photodiode signal. The photocurrent is amplified by a low-noise current preamplifier (SR570). Since different noise frequencies could be observed in the measured data, the laser diode is modulated with a frequency of 1kHz using a function generator (HP 33120A). The modulated photocurrent is compared and filtered with this reference frequency by a lock-in amplifier (SR830).

To achieve reproducible polarization conditions in the fibers, all the fiber patch cords have been fixed in position. The positions of the polarization controller's paddles could be restored with a custom angle scale. Therefore, the polarization state of the light that is coupled into the exchangeable bare fiber is reproducible. In order to reduce the effect of polarization change due to propagation through the bare fiber, all fibers were cut to the same length and the positions of the fiber clamps' pressure points are aligned with custom alignment scales to the same distances with respect to the fiber tips. Small changes of the polarization can be compensated by slightly varying the polarization controller's paddles, while observing the intensity transmitted into the forward direction. After following the procedure described, changes in polarization were found to be very small.

5. Results

Initially, only the total-internal-reflection prism was written on a fiber tip to ensure that the total internal reflection is independent of the incident polarization. Figure 6(a) shows a colored scanning electron micrograph of the prism structure on the fiber's facet. We characterized the transmission (Fig. 7) and found that the angular intensity distribution is nearly independent of the polarization setting and contains only a low amount of stray light.

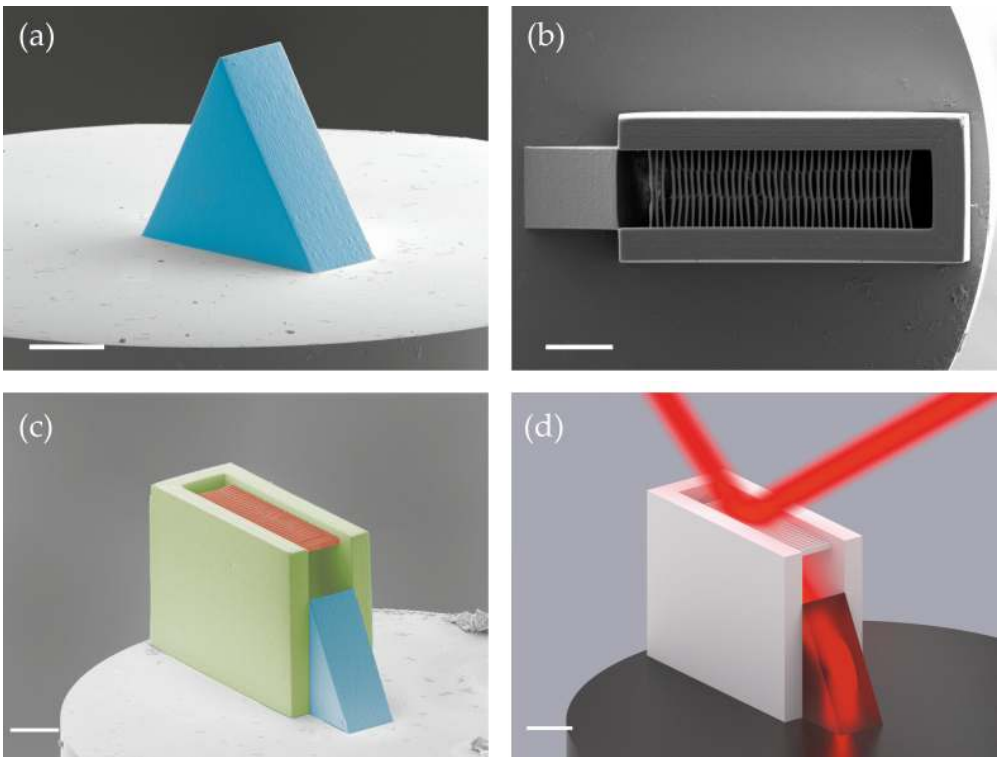

Fig. 6. (a) Colored scanning electron micrograph of a fiber with a total-internal-reflection prism on its end facet. (b) Top view scanning electron micrograph of the polarizing beam splitter on a fiber facet. (c) Colored scanning electron micrograph of the same structure, with the prism highlighted in blue, the lamellar grating in red, and the supporting structure in green. (d) Rendered view of the structure in operation. All scale bars are $10\mu m$.

Optics EXPRESS

A top-view scanning electron micrograph of the complete polarizing beam splitter structure is depicted in Fig. 6(b). We have randomly selected 10 lamellae and measured their width. We find a mean of 370 nm and a standard deviation of 33 nm. Within the sensitivity with respect to deviations described in section 3, the measured mean value is sufficiently close to the design value of 373 nm (see Table 1). However, the lamellae show some deformation. We reiterate that the grating is suspended at an elevated height and that its lamellae have an aspect close to 5, making the fabrication challenging. The results shown have been obtained after a tedious and long experimental optimization procedure. A side-view of the entire structure is depicted in Fig. 6(c). To allow for a direct comparison, the rendered view in Fig. 6(d) illustrates the operation principle.

The device was tested by launching linearly polarized light ($0°$ and $90°$ polarization with respect to the horizontal) into the fiber. For each setting of the polarization controller, the full $180°$ range is probed and plotted in Fig. 8. The grating efficiency, defined as the intensity guided into the desired order with respect to total incident intensity, is 92% for the TM and 80% for the TE mode. The resulting degree of polarization is 81% and 82% respectively. The width of the peaks is mainly governed by the numerical aperture of the detection telescope.

As expected, the total intensity of the TM polarized component is considerably higher than the TE polarized component's intensity, since, in contrast to the TE polarization, the TM polarized light is not significantly affected by the grating. The total intensity of the TE polarization is reduced about 40%, caused by the reflection at the lamellar grating, which can be seen in the simulations (see Fig. 4), scattering losses due to structural imperfections, and the slightly less efficient TE transmission of the prism (see Fig. 7).

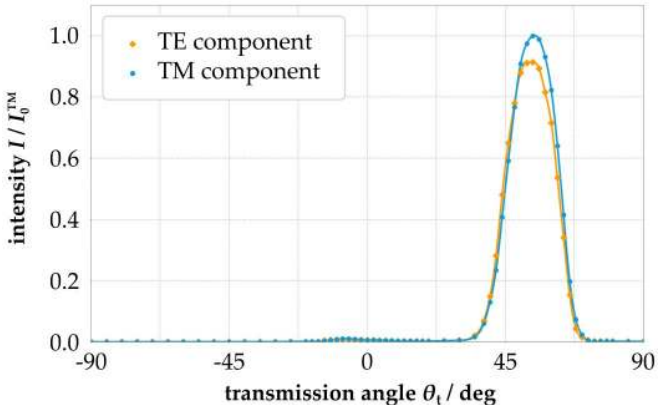

Fig. 7. Angular intensity distribution for TE and TM polarization directions and for a fiber with only the totally internal reflecting prism printed on its facet (compare Fig. 6(a)).

Furthermore, our results show that the TE polarized light is diffracted at an angle close to $-45°$, rather than the design value of $-56.3°$. The transmission angle θ_t of TE-polarized light will not be equal to the angle of the incident light θ_i, in the event the illumination does not satisfy the Littrow condition. At this point, we note that the Littrow angle was calculated for a period of $0.932\,\mu m$ but the period written was somewhat larger and, therefore, the slightly different diffraction angle is not surprising.

Optics EXPRESS

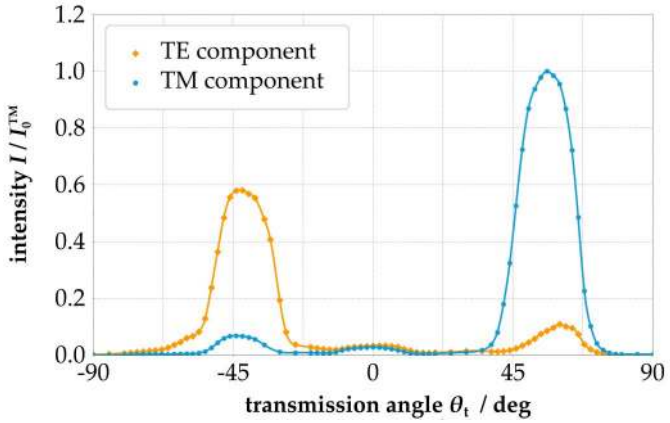

Fig. 8. Transmitted intensity for both polarization directions after the polarizing beam splitter (compare structure shown in Fig. 6(c) and rendering in Fig. 6(d)).

6. Conclusions

In this paper, we have designed by modal theory and finite-element calculations, fabricated by 3D direct laser writing, and characterized experimentally at 1550 nm wavelength, a polarizing beam splitter integrated directly onto the end facet of a single-mode optical fiber. This integrated element includes a refractive prism, which we intentionally slightly displace from the center of the fiber mode, and a polarization-dependent sub-wavelength grating, composed of suspended high-aspect ratio lamellae. The experimental characterization is in good agreement with theory, despite the slight distortion of the lamellae. We find a polarization purity exceeding 80% for both emerging beams.

Funding

Excellence Cluster "3D Matter Made to Order (3DMM2O)"; Helmholtz program "Science and Technology of Nanosystems (STN)"; KIT Nanostructure Service Laboratory (NSL); Karlsruhe School of Optics and Photonics (KSOP); Alexander von Humboldt Foundation.

Acknowledgments

SB would like to thank the Alexander von Humboldt Foundation for supporting her stay at the Institute of Applied Physics (APH) at KIT. We thank Johann Westhauser (KIT) for help in the construction of the fabrication setup.

References

1. G. Kostovski, P. R. Stoddart, and A. Mitchell, "The optical fiber tip: an inherently light-coupled microscopic platform for micro- and nanotechnologies," Adv. Mater. **26**(23), 3798–3820 (2014).
2. M. Prasciolu, D. Cojoc, S. Cabrini, L. Businaro, P. Candeloro, M. Tormen, R. Kumar, C. Liberale, V. Degiorgio, A. Gerardino, G. Gigli, D. Pisignano, E. Di Fabrizio, and R. Cingolani, "Design and fabrication of on-fiber diffractive elements for fiber-waveguide coupling by means of e-beam lithography," Microelectron. Eng. **67–68**, 169–174 (2003).
3. N. Wang, M. Zeisberger, U. Hübner, and M. A. Schmidt, "Nanotrimer enhanced optical fiber tips implemented by electron beam lithography," Opt. Mater. Express **8**(8), 2246 (2018).
4. M. Vanek, J. Vanis, Y. Baravets, F. Todorov, J. Ctyroky, and P. Honzatko, "High-power fiber laser with a polarizing diffraction grating milled on the facet of an optical fiber," Opt. Express **24**(26), 30225–30233 (2016).
5. F. Schiappelli, R. Kumar, M. Prasciolu, D. Cojoc, S. Cabrini, M. De Vittorio, G. Visimberga, A. Gerardino, V. Degiorgio, and E. Di Fabrizio, "Efficient fiber-to-waveguide coupling by a lens on the end of the optical fiber fabricated by focused ion beam milling," Microelectron. Eng. **73–74**, 397–404 (2004).
6. S. Cabrini, C. Liberale, D. Cojoc, A. Carpentiero, M. Prasciolu, S. Mora, V. Degiorgio, F. De Angelis, and E. Di Fabrizio, "Axicon lens on optical fiber forming optical tweezers, made by focused ion beam milling," Microelectron. Eng. **83**(4-9), 804–807 (2006).

Optics EXPRESS

7. P. Vayalamkuzhi, S. Bhattacharya, U. Eigenthaler, K. Keskinbora, C. T. Samlan, M. Hirscher, J. P. Spatz, and N. K. Viswanathan, "Direct patterning of vortex generators on a fiber tip using a focused ion beam," Opt. Lett. **41**(10), 2133–2136 (2016).
8. K. Weber, F. Hütt, S. Thiele, T. Gissibl, A. Herkommer, and H. Giessen, "Single mode fiber based delivery of OAM light by 3D direct laser writing," Opt. Express **25**(17), 19672–19679 (2017).
9. T. Baldacchini, *Three-dimensional microfabrication using two-photon polymerization* (Elsevier, 2016).
10. H. E. Williams, D. J. Freppon, S. M. Kuebler, R. C. Rumpf, and M. A. Melino, "Fabrication of three-dimensional micro-photonic structures on the tip of optical fibers using SU-8," Opt. Express **19**(23), 22910–22922 (2011).
11. C. Liberale, G. Cojoc, P. Candeloro, G. Das, F. Gentile, F. De Angelis, and E. Di Fabrizio, "Micro-optics fabrication on top of optical fibers using two-photon lithography," IEEE Photonics Technol. Lett. **22**(7), 474–476 (2010).
12. C. Liberale, G. Cojoc, F. Bragheri, P. Minzioni, G. Perozziello, R. La Rocca, L. Ferrara, V. Rajamanickam, E. Di Fabrizio, and I. Cristiani, "Integrated microfluidic device for single-cell trapping and spectroscopy," Sci. Rep. **3**(1), 1258 (2013).
13. T. Gissibl, S. Thiele, A. Herkommer, and H. Giessen, "Two-photon direct laser writing of ultracompact multi-lens objectives," Nat. Photonics **10**(8), 554–560 (2016).
14. T. Gissibl, M. Schmid, and H. Giessen, "Spatial beam intensity shaping using phase masks on single-mode optical fibers fabricated by femtosecond direct laser writing," Optica **3**(4), 448 (2016).
15. M. Kowalczyk, J. Haberko, and P. Wasylczyk, "Microstructured gradient-index antireflective coating fabricated on a fiber tip with direct laser writing," Opt. Express **22**(10), 12545–12550 (2014).
16. A. Wickberg, J. B. Mueller, Y. J. Mange, J. Fischer, T. Nann, and M. Wegener, "Three-dimensional micro-printing of temperature sensors based on up-conversion luminescence," Appl. Phys. Lett. **106**(13), 133103 (2015).
17. J. Feng, C. Zhou, J. Zheng, H. Cao, and P. Lv, "Dual-function beam splitter of a subwavelength fused-silica grating," Appl. Opt. **48**(14), 2697–2701 (2009).
18. P. Vayalamkuzhi, G. M. Sridharan, and S. Bhattacharya, "Subwavelength transmission gratings for polarization separation in the infrared," JM3," JMMMGF **15**(2), 023504 (2016).
19. M. Thiel, M. Hermatschweiler, M. Wegener, and G. von Freymann, "Thin-film polarizer based on a one-dimensional–three-dimensional–one-dimensional photonic crystal heterostructure," Appl. Phys. Lett. **91**(12), 123515 (2007).
20. T. Bückmann, N. Stenger, M. Kadic, J. Kaschke, A. Frölich, T. Kennerknecht, C. Eberl, M. Thiel, and M. Wegener, "Tailored 3D mechanical metamaterials made by dip-in direct-laser-writing optical lithography," Adv. Mater. **24**(20), 2710–2714 (2012).